Hypoxic induction of vascular endothelial growth factor regulates murine hematopoietic stem cell function in the low-oxygenic niche.

Rehn, Matilda; Olsson, André; Reckzeh, Kristian; Diffner, Eva; Landberg, Göran; Cammenga, Jörg

Published in:
Blood

DOI:
10.1182/blood-2011-01-332890

2011

Hypoxic Induction of Vascular Endothelial Growth Factor Regulates Murine Hematopoietic Stem Cell Function in the Low-oxygenic Niche.

Matilda Rehn[1] , André Olsson[1] , Kristian Reckzeh[1] , Eva Diffner[3], Peter Carmeliet[4,5], Göran Landberg[3], Jörg Cammenga[1, 2]

1. Division of Molecular Medicine and Gene Therapy, Lund Stem Cell Center, Lund University, Lund, Sweden.
2. Department of Hematology, Skåne University Hospital, Lund, Sweden.
3. Center for Molecular Pathology, Skåne University Hospital, Malmö, Sweden.
4. Laboratory of Angiogenesis and Neurovascular Link, Vesalius Research Center (VRC), VIB, Leuven, Belgium.
5. Laboratory of Angiogenesis and Neurovascular Link, Vesalius Research Center (VRC), K.U.Leuven, Leuven, Belgium.

Corresponding author: Jörg Cammenga, Molecular Medicine and Gene Therapy, BMC A12, 22184 Lund, Sweden; e-mail: jorg.cammenga@med.lu.se; phone: +46-46-2221446; fax: +46-46-2220568.

Abstract

Hypoxia is emerging as an important characteristic of the hematopoietic stem cell (HSC) niche, but the molecular mechanisms contributing to quiescence, self-renewal, and survival remain elusive. Vascular endothelial growth factor A (VEGFA) is a key regulator of angiogenesis and hematopoiesis. Its expression is commonly regulated by hypoxia-inducible factors (HIF) that are functionally induced in low-oxygen conditions and that activate transcription by binding to hypoxia-response elements (HRE). *Vegfa* is indispensable for HSC survival, mediated by a cell-intrinsic, autocrine mechanism. We hypothesized that a hypoxic HSC microenvironment is required for maintenance or upregulation of *Vegfa* expression in HSCs and therefore crucial for HSC survival. We have tested this hypothesis in the mouse model *Vegfa*$^{\delta/\delta}$, where the HRE in the *Vegfa* promoter is mutated, preventing HIF binding. *Vegfa* expression was reduced in highly purified HSCs from *Vegfa*$^{\delta/\delta}$ mice, showing that HSCs reside in hypoxic areas. Loss of hypoxia-regulated *Vegfa* expression increases the numbers of phenotypically defined hematopoietic stem and progenitor cells. However, HSC function was clearly impaired when assessed in competitive transplantation assays. Our data provide further evidence that HSCs reside in a hypoxic microenvironment and demonstrate a novel way in which the hypoxic niche affects HSC fate, via the hypoxia-*Vegfa* axis.

Introduction

The process of blood formation originates with the hematopoietic stem cell (HSC) which is responsible for the life-long supply of mature blood cells through the unique ability to combine self-renewal and differentiation. During the later stages of mammal development, HSCs are present in the fetal liver (FL) from where they seed the bone marrow (BM), which remains the main site of hematopoiesis throughout adult life. The *HSC niche* is a term used to describe the location and regulatory microenvironment of HSCs. In the BM, cellular HSC niche components include bone-forming osteoblasts [1-2] and perivascular cells [3-4], that through production of various secreted factors as well as through direct cell-cell interactions can affect HSC behavior. As for location it is thought that

HSCs are present at a higher frequency at the endosteum close to the bone surface, since *ex vivo* labeled HSCs tend to localize to the endosteal areas of the BM [5-6]. However, within these areas HSCs are likely to associate with both osteoblastic and sinusoidal endothelial cells [7]. The FL HSC niche is much less defined than that in the BM, but a candidate FL niche component is a $CD3^+$ $Ter119^-$ population that can provide HSC support [8].

Apart from HSC regulatory cues such as cell-cell contact and production of soluble factors, it is possible that variations in oxygen availability can affect HSCs, and it has been hypothesized that hypoxia is a characteristic of the HSC niche [9]. Oxygen levels are generally lower in BM compared to peripheral blood (PB) [10]. Two studies have demonstrated that fractions of BM that were not well perfused by injected Hoechst dye, an indirect measure of oxygen availability, were also the fractions that showed the highest HSC activity in transplantation assays [11-12]. Similarly, by assuming that low levels of reactive-oxygen species (ROS) corresponds to low levels of oxygen, it was shown that BM cell populations with low ROS activity have higher HSC potential compared to populations where ROS activity is high [13]. Moreover, the HSC enriched endosteal areas of BM are positively stained for the hypoxic marker Pimonidazol [14], as are long-label-retaining cells with a sinusoidal location [15]. In addition, a number of studies have shown that both human and murine hematopoietic stem and progenitor cell (HSPC) proliferation and differentiation can be affected by hypoxic treatment *ex vivo* [9,16-22]. Cells exposed to hypoxia generally respond by induction of Hypoxia-Inducible Factors (HIF) HIF-1 and/or HIF-2 [23-25]. HIFs are transcription factors that consist of two subunits: a HIF-α subunit (HIF1A, EPAS1 or HIF3A) that associates with HIF-β (also known as ARNT1). The activity of HIFs is post-translationally regulated in such a way that the α-subunit is degraded in normoxia due to the action of oxygen-sensing prolyl-hydroxylase-domain proteins. This leads to binding by the E3-ubiqutin-ligase complex von Hippel Lindau (VHL), subsequently leading to proteasomal degradation of the subunit [26-28]. In situations of hypoxia this process is no longer active, allowing HIF-α and HIF-β subunits to form heterodimers that can bind to hypoxia-response elements (HRE) in promoters and activate transcription of target genes [24]. HIF-1α was recently shown to be an important regulator of HSCs in the hypoxic niche. Loss of HIF-1α activity in HSCs was associated with increased cycling and exhaustion of stem cell activity upon secondary transplantation, while stabilization of HIF-1α by deletion of VHL led to a marked reduction in HSC cycling [29]. Consistent with these findings, we have shown that *in vitro* hypoxic culture as well as chemical or retroviral stabilization of HIF-1α leads to reduced cycling of HSPCs [30]. Apart from regulating HSC quiescence, oxygen availability and HIF activity may affect hematopoiesis in other ways yet unknown.

Vascular endothelial growth factor A (VEGFA) is a well-known angiogenic factor that is induced by hypoxia [31-32]. Complete absence or haploinsufficiency of *Vegfa* during development causes embryonic lethality due to a failure to establish vascular angiogenesis as well as hematopoiesis [33-34]. *Vegfa* is also absolutely required for adult hematopoiesis. By conditional deletion of the *Vegfa* gene in the hematopoietic system, Gerber *et al*. could show that *Vegfa* is necessary for maintenance of BM activity. Furthermore *Vegfa*-deficient HSCs fail to engraft lethally irradiated mice despite the presence of VEGFA in the microenvironment of the recipients, demonstrating a cell-intrinsic effect of VEGFA on HSCs. This effect was shown to be regulated by an internal, autocrine loop since antibodies blocking VEGF-receptor activity on the cell surface did not lead to any effect on *in vitro* colony formation, whereas intracellular inhibitors of VEGF-signal transduction caused apoptosis [35]. In addition to the HSC intrinsic effect, VEGFA may also regulate HSC function via extrinsic mechanisms. Establishment of HSC osteoblastic niches via endochondral ossification was shown to depend on VEGFA availability [36]. Furthermore, engraftment of transplanted HSCs is dependent on proper expression of a VEGF-receptor, *Kdr*, in the irradiated BM [37].

We hypothesized that a potential role of the hypoxic HSC niche is to up-regulate *Vegfa* expression in HSCs, thereby contributing to HSC survival. To test this hypothesis we have investigated the hematopoietic phenotype in a model where hypoxia-regulated *Vegfa* expression is abrogated. In $Vegfa^{\delta/\delta}$ mice, the HRE in the *Vegfa* promoter has been deleted at both alleles, thereby inhibiting HIF-binding and subsequent activation of *Vegfa* expression following hypoxia[38]. *Vegfa* expression is reduced in highly purified HSCs from BM of $Vegfa^{\delta/\delta}$ mice but not in mature cells. This observation provides further support for the hypothesis that HSCs reside in hypoxic locations of BM. We show that ablation of the hypoxic regulation of *Vegfa* expression within the hematopoietic system affects hematopoietic differentiation and increases the number of phenotypically identified HSCs, but

at the same time leads to a functional defect of HSCs identified by competitive transplantation experiments.

Material & Methods

Mice

Vegfa^{tm2Pec} mice [38] (referred to as *Vegfa*$^{\delta}$) were kindly provided by P. Carmeliet, Leuven University, Belgium. *Vegfa*$^{\delta/+}$ on a mixed 129 SvS6 x Swiss Tac background (CD45.2) were intercrossed with C57Bl/6J (CD45.2) wild type (wt) mice. F_1 *Vegfa*$^{\delta/+}$ mice from this crossing were mated to obtain mice and fetal livers with the *Vegfa*$^{\delta/\delta}$ genotype. Wt littermates were used as controls in all experiments. The colony was maintained on a C57Bl/6J x 129 SvS6 x Swiss Tac mixed background. On this background, the mice had a mixed genotype at the H2-locus (*H2b/H2q*). For BM transfer experiments, mice were therefore bred to obtain a homozygous *H2b/H2b* genotype, compatible with C57Bl/6 and B6.SJL used as recipients and source of competitor cells. *Vegfa*$^{\delta/\delta}$ mice display a partial prenatal lethality and adult *Vegfa*$^{\delta/\delta}$ mice that survive develop an amyotrophic lateral sclerosis-like disease around 6 months. In our study we analyzed mice before the onset of disease, to avoid any unspecific effects on the hematopoietic system.

Flow Cytometry

For a full list of antibody clones, see Supplementary material. For analysis of chimerism in transplanted mice, PB and BM were stained with CD45.1-PerCp and CD45.2-FITC. To detect B-cells, T-cells, and myeloid cells, samples were stained with B220-PE, B220-APC, CD3-PE, and Mac-1-APC. For analysis of the lineage$^-$, Sca-1$^+$, c-kit$^+$ (LSK) compartment in the BM, samples were first stained for lineage-specific markers by unconjugated antibodies against B220, CD3, CD4, CD8, Ter119, Mac-1, and Gr-1 followed by Tricolor-conjugated goat anti–rat antibodies (Invitrogen, Carlsbad, CA) and Sca-1-PE, c-kit-APC and CD34-FITC. For purification of LSK CD34$^{+/-}$ cells, samples were enriched for c-kit expression prior to staining using MidiMACS columns (Miltenyi, Bergisch Gladbach, Germany). For analysis of ROS content, pre-stained cells were incubated in 10 µM 2′,7′-Dichlorofluorescin diacetate (DCFDA) (Sigma-Aldrich, St. Louis, MO) for 20 min at 37 °C. For analysis of the LSK compartment in FL, samples were first depleted of Ter119$^+$ cells and thereafter stained for the lineage-specific markers B220, CD5, CD8, Ter119, and Gr-1 followed by Tricolor-conjugated goat anti–rat and Sca-1-FITC, c-kit-APC, and CD150-APC. Cells were analyzed or sorted using a FACS CantoII, FACS Calibur, FACS Diva or FACS Aria (BD Bioscience, San Jose, CA) and FlowJo software (Tree Star Software, San Carlos, CA). Total blood counts were measured by automated hematocytometry on a Sysmex system (Sysmex GmbH, Kungsbacka Sweden).

Competitive-repopulation Assay

Recipient mice, 8–12 weeks old, (C57Bl/6 x B6.SJL; CD45.1/2) were lethally irradiated with 900 cGy 20–24 hours prior to transplantation. 2x10^5 BM cells from *Vegfa*$^{\delta/\delta}$ or wt (CD45.2) mice were mixed with 2x10^5 competitor BM cells from B6.SJL (CD45.1) mice and injected into the tail vein of irradiated recipients. Peripheral-blood chimerism was measured by FACS analysis of CD45.1 and CD45.2 cell surface expression at 4, 8, 12, and 15 weeks post transplantation. At 15 weeks, chimerism in the BM LSK compartment was analyzed. For quantification of competitive repopulating units (CRU), groups of recipient mice were transplanted with 5x10^3, 2x10^4, 5x10^4, and 2x10^5 BM cells from *Vegfa*$^{\delta/\delta}$ or wt mice together with 2x10^5 competitor cells. Positive engraftment was defined as more than 1% lymphoid and myeloid engraftment at 22 weeks post transplantation. CRU content was analyzed using L-calc software (STEMCELL Technologies, Vancouver).

Statistics

Statistical significance was determined by calculating two-tailed p-values using t test or Mann-Whitney test.

Results

Vegfa Expression Is Reduced in HSCs from *Vegfa*$^{\delta/\delta}$ Mice

To investigate whether hypoxia-induced *Vegfa* expression was indeed perturbed in the hematopoietic system of *Vegfa*$^{\delta/\delta}$ mice, we incubated c-kit^{+} cells from wt or *Vegfa*$^{\delta/\delta}$ mice in normoxic or hypoxic conditions and thereafter measured *Vegfa* expression by quantitative real-time PCR (Q-RT-PCR). *Vegfa* expression was increased in wt cells exposed to hypoxia when compared to normoxic expression levels. At the same time, *Vegfa* expression remained largely unchanged in *Vegfa*$^{\delta/\delta}$ cells upon hypoxic exposure (Figure 1E). We also measured expression of *Pgk1* and *Hk2*, two glycolysis-associated genes previously reported to be induced by hypoxia [39]. Expression of these two genes was increased in both genotypes after hypoxic culture, demonstrating the specificity of the lacking *Vegfa* induction in *Vegfa*$^{\delta/\delta}$ mice (Figure 1 F-G). We next measured *Vegfa* expression in different BM cell populations. In total BM cells, c-kit^{+}, and LSK CD34^{+} cells, there were no differences in *Vegfa* expression between wt and *Vegfa*$^{\delta/\delta}$, arguing for the fact that these subsets have similar basal expression but lack hypoxia/HIF-induced up-regulation of *Vegfa* (Figure 1A-C). However, in LSK CD34^{-} cells, a population highly enriched for long-term repopulating HSCs, *Vegfa* expression was significantly lower in *Vegfa*$^{\delta/\delta}$ samples compared to wt (Figure 1D). These results indirectly indicate that HSCs are localized in hypoxic areas where *Vegfa* expression is induced, while more mature cells are not.

Endochondral Ossification Is Impaired in *Vegfa*$^{\delta/\delta}$ Mice while BM Morphology and Microvessel Density Are not Affected

Apart from hematopoiesis, VEGFA is involved in processes like angiogenesis and endochondral ossification. Since both bone-associated and vascular-associated HSC niches have been proposed, we wanted to investigate if the bone or BM vascular architecture was affected by the *Vegfa*$^{\delta/\delta}$ mutation because such changes could cause secondary effects on hematopoiesis by altering the HSC niche. BM sections from femur of *Vegfa*$^{\delta/\delta}$ mice appeared normal with comparable BM cellularity and distribution of bone trabeculae compared to wt sections. However, the epiphyseal growth plate in the femur of young, but not adult, *Vegfa*$^{\delta/\delta}$ mice was reduced compared to wt, suggesting a defect in endochondral bone formation (Figure 2A, D). Sections of bone were stained with antibodies against vWF to visualize distribution of microvessels. No differences in microvessel density could be observed between the two genotypes (Figure 2B-C).

Vegfa$^{\delta/\delta}$ Mice Have Anemia and Altered Numbers of Differentiated Cells in the BM

To investigate the effect of ablated hypoxia-regulated *Vegfa* expression on hematopoietic output, we measured WBCs, platelets, RBCs, hemoglobin, and hematocrit in the PB of wt and *Vegfa*$^{\delta/\delta}$ mice. WBC and platelet counts were not significantly different between the groups (Figure 3A-B). However, RBC, hemoglobin, and hematocrit values were reduced in the PB of *Vegfa*$^{\delta/\delta}$ mice compared to wt littermates, suggesting a deficiency in erythropoiesis (Figure 3C-E). When erythroid blast forming unit (BFU-E) formation in response to recombinant erythropoietin was assessed *in vitro*, we could not detect any deficiency in *Vegfa*$^{\delta/\delta}$ cells (Supplementary Figure 1D). To investigate whether erythropoietic development was blocked at a specific stage, we performed FACS analysis using markers defining maturing erythrocytes. We found that proerythroblasts and basophilic erythroblasts were slightly increased in the BM of *Vegfa*$^{\delta/\delta}$ mice, while the later stages (late baso- and chromatophilic erythroblasts and orthochromatic normoblasts) tended to be decreased (Supplementary Figure 1A-C). To investigate differentiation capacity towards lymphoid and myeloid lineages, FACS analysis for B-cells (B220^{+}), T-cells (CD3^{+}), and monocytes (Mac-1^{+}) was performed. We observed a slight increase in T-cells and a decrease in B-cell and monocyte numbers in the BM of *Vegfa*$^{\delta/\delta}$ mice compared to wt (Figure 3G-H), while there were no differences in lineage distribution in the PB (Figure 3F).

Ablated Hypoxia-regulated *Vegfa* Expression Increases Adult HSPC Frequency

To determine whether hypoxia-related *Vegfa* expression is needed to maintain HSPC integrity, we measured the frequency of different cell populations in the BM of wt and *Vegfa*$^{\delta/\delta}$ mice. Total BM cellularity was slightly but significantly decreased in *Vegfa*$^{\delta/\delta}$ mice compared to wt (Figure 4A). Hematopoietic colony forming unit (CFU) activity *in vitro* was similar between cells from wt and

Vegfa$^{\delta/\delta}$ BM (Figure 4B). Recombinant VEGFA was added to the cultures with the intent to rescue a possible defect in CFU-formation, but the addition of the protein does not seem to have any effect on colony formation by itself. CFU assays were also performed in hypoxic conditions (1% O_2). Although it has previously been reported that hypoxia can increase colony formation [19-20], we did not detect any major changes compared to normoxia (Figure 4B). FACS analysis showed that the frequency and total numbers of LSK cells in BM of *Vegfa*$^{\delta/\delta}$ mice were not different between the genotypes (Figure 4C-E). The frequency of cells in the LSK CD34$^-$ compartment was slightly increased in contrary to our hypothesis, but total numbers were not (Figure 4F-H).

Ablated Hypoxia-regulated *Vegfa* Expression Causes Late Gestational Lethality and Increases HSPC Frequency in the FL

The *Vegfa*$^{\delta/\delta}$ mutation is partly embryonically lethal for still unknown reasons. We therefore wanted to investigate the time point at which embryos die *in utero* to evaluate the possibility that the lethality is associated with the time point of FL hematopoiesis or BM seeding. Prenatal lethality was previously reported to be approximately 60% in mice on 129 SvS6 x Swiss Tac background [38]. This number was increased in our hands, where an additional element of the C57Bl/6 strain has been added, and reached 76%. In addition, we observed that back-crossing further than one generation to C57Bl/6 led to a complete absence of homozygous pups born from δ/+ x δ/+ matings (100% lethality). By comparing genotype outcomes from mice surviving past birth to embryos killed at day 15.5 of embryogenesis, we could observe that the frequency of the δ/δ genotype was higher, although not reaching mendelian ratios, at day 15.5 compared to post-birth time points (18% and 6% respectively) (Table 1), suggesting substantial lethality during the late gestational period. To investigate whether hypoxia-regulated *Vegfa* expression is needed to maintain FL hematopoiesis, we measured the frequencies of HSPCs in FLs of wt and *Vegfa*$^{\delta/\delta}$ mice. Consistent with the BM findings, cellularity was significantly lower in *Vegfa*$^{\delta/\delta}$ FLs compared to wt (Figure 5A). CFU activity was similar between the two genotypes (Figure 5B). By FACS analysis, we detected an increase in the frequency of LSK cells, but not absolute numbers, in *Vegfa*$^{\delta/\delta}$ FLs compared to wt (Figure 5C-E). The LSK CD150$^+$ frequency, but not absolute numbers, was increased in *Vegfa*$^{\delta/\delta}$ FLs (Figure 5F-H).

HSCs Lacking Hypoxia-regulated *Vegfa* Expression Have Impaired Competitive-repopulation Capacity

To evaluate HSC function, we performed competitive-repopulation assays, where $2x10^5$ BM cells from wt or *Vegfa*$^{\delta/\delta}$ mice were transferred to lethally irradiated recipient mice together with an equal dose of BM competitor cells from CD45 congenic mice. Both short-term and long-term reconstitution was significantly reduced in PB of recipients of *Vegfa*$^{\delta/\delta}$ BM compared to wt, indicating HSC impairment (Figure 6A-C). Engrafted cells from wt and *Vegfa*$^{\delta/\delta}$ mice showed comparable contribution to myeloid and lymphoid lineages (Figure 6D). After 15 weeks we evaluated chimerism in the BM LSK compartment of recipient mice. The levels of CD45.2-expressing LSK cells were significantly decreased in recipients of *Vegfa*$^{\delta/\delta}$ BM, confirming that HSCs lacking hypoxic *Vegfa* expression have defect engraftment ability (Figure 6E). Furthermore, a CRU assay where limiting doses of BM cells were transplanted to groups of recipients, showed that CRU frequency was approximately 3-fold lower in BM from *Vegfa*$^{\delta/\delta}$ mice compared to wt ($1/1.1x10^5$ and $1/3.7x10^4$ respectively) (Figure 6F).

Increased HSC Frequency in *Vegfa*$^{\delta/\delta}$ Mice Is not Due to Selective Expansion of a Subpopulation of Normoxic HSCs

The unexpected finding of increased HSC frequency as defined by surface markers in BM of *Vegfa*$^{\delta/\delta}$ mice may reflect a situation of stressed hematopoiesis since RBC output is lower and HSC function is clearly impaired. Therefore we wanted to investigate whether this increase is due to expansion of a subpopulation of HSCs that reside in normoxia and thereby are able to escape the drastic effect of a non-functional hypoxic *Vegfa* induction. To this end we measured *Vegfa* levels in LSK CD34$^-$ cells that were further subdivided based on ROS content, measured by DCFDA staining. Since ROS are formed as a consequence of oxygen dependent reactions, ROS levels are assumed to correlate with oxygen availability. We used this approach to divide the LSK CD34$^-$ compartment into hypoxic (ROS^{lo}) and normoxic (ROS^{hi}) populations (Figure 7A). Distinct ROS^{lo} and ROS^{hi} populations were detected in both *Vegfa*$^{\delta/\delta}$ and wt mice. There was a trend towards an increase in the ROS^{hi} CD34$^-$

population as well as the ROS^{lo} CD34^{-} population in *Vegfa*$^{\delta/\delta}$ mice compared to wt but the changes were not statistically significant (Figure 7A-B). When we measured *Vegfa* gene expression in the sorted subpopulations, we again detected lower *Vegfa* expression in both ROS^{lo} CD34^{-} and ROS^{hi} CD34^{-} *Vegfa*$^{\delta/\delta}$ samples compared to wt, suggesting relatively hypoxic locations for both populations (Figure 7C).

Discussion

Several pieces of evidence for the existence of BM HSC niches low in oxygen have been presented, but the importance of such areas to HSC fate has only begun to be elucidated. It is clear that hypoxia, indirectly measured by low ROS-activity [13], low perfusion as measured by uptake of injected Hoechst dye [11-12], or low metabolic activity [40], correlates with increased HSC activity. Indeed, these findings fit with the idea that HSCs, in order to last for a complete life-time, need to be preserved from stress imposed by potentially mutagenic molecules that are bi-products of oxygen consumption. Recent data demonstrate an important role for HIF-1α in HSC function. HSCs lacking expression of *Hif1a* are able to engraft lethally irradiated recipients but fail to sustain hematopoiesis for extended periods or after serial transplantation, indicating exhaustion from extensive proliferation [29]. In agreement with this, we have shown that *in vitro* hypoxic treatment or constitutive activation of HIF-1α activity in HSCs reduces proliferation and leads to up-regulation of cell cycle-inhibitory genes [30]. Thus, one important function of the hypoxic niche seems to be keeping HSCs in relative quiescence. However, since HIF-1α is such a master regulator of the hypoxic response with hundreds of known target genes, it is tempting to believe that there are other ways in which hypoxia affects HSC fate. Although being one of the typical hypoxia-regulated genes as shown in several tissues, the importance of the hypoxia-VEGFA axis in HSC biology has never been examined. Because HSCs likely reside in a hypoxic microenvironment, and since *Vegfa* is a highly hypoxia-dependent gene crucial for HSC survival, we hypothesized that abrogated hypoxia-induced expression in our model would affect HSC numbers and/or function.

Q-RT-PCR experiments showed that *Vegfa* expression in wt cells was lowest in unfractionated BM but increased in the more primitive c-kit^{+}, LSK CD34^{+}, and LSK CD34^{-} populations. In purified HSCs from *Vegfa*$^{\delta/\delta}$ mice, where hypoxia is not able to affect *Vegfa* expression, *Vegfa* was reduced compared to wt control cells. The reduction was specifically seen in the LSK CD34^{-} population and thus demonstrates that long-term HSCs reside in hypoxic areas of BM while more mature cells are not. Whether these areas are preferentially endosteal, vascular or other, cannot be concluded from our data.

Differentiation towards myeloid, B-cell and T-cell lineages as measured by FACS was normal in PB of *Vegfa*$^{\delta/\delta}$ mice, while in BM a slightly distorted distribution was observed. *Vegfa*$^{\delta/\delta}$ mice are slightly anemic with lower levels of RBCs, hemoglobin, and hematocrit in the PB compared to wt. FACS analysis of progenitors at different stages of erythropoiesis showed slightly lower levels of late developing erythroblasts with a corresponding increase in the earlier progenitor populations: proerythroblasts and basophilic erythroblasts. Furthermore, the more primitive BFU-E, as measured by colony formation in response to erythropoietin *in vitro*, was normal. It is therefore possible that the decreased levels of peripheral RBCs in *Vegfa*$^{\delta/\delta}$ mice is due to a general survival defect of late erythrocytes that is dependent on hypoxia-induced *Vegfa*. *Vegfa*$^{\delta/\delta}$ mice have lower numbers of BM cells compared to wt littermates. However, the BM did not appear hypocellular in histological sections and therefore the decreased BM count is probably rather a secondary effect of the smaller overall size of *Vegfa*$^{\delta/\delta}$ mice compared to their wt littermates than a direct effect on hematopoiesis. The frequency of phenotypically defined long-term HSCs, LSK CD34^{-} cells, are increased in BM of *Vegfa*$^{\delta/\delta}$ mice, in contrary to our hypothesis that ablated hypoxic *Vegfa* up-regulation would decrease HSC numbers. However, phenotypically defined HSCs do not necessarily correspond to functionally defined HSCs. This unanticipated phenomenon has been observed in other transgenic mice lacking genes important in HSC function like *Gfi1* and *Cxcr4* [41-42]. One way to interpret the data is that the increased frequency of HSCs in *Vegfa*$^{\delta/\delta}$ mice is a way to compensate for less functional ones. This is in agreement with the results that we obtained from the HSC functional assays, where HSCs from *Vegfa*$^{\delta/\delta}$ mice were shown to have a lower capacity to competitively reconstitute irradiated hosts compared to wt HSCs. The

effect was seen as early as 4 weeks but was more pronounced at 15 weeks post transplantation, showing that short-term and more importantly long-term reconstitution was affected. In addition, *Vegfa*$^{\delta/\delta}$ contribution to the LSK compartment at 15 weeks was reduced while wt chimerism was high. Although equal doses of test and competitor cells were transplanted, wt chimerism was higher than the expected 50%. However, wt test cells in our experiment are likely to compete better than the competitor cells due to their 129Sv background; It has been demonstrated that 129Sv mice have increased HSC activity compared to B6 strains [43]. The engraftment defect of *Vegfa*$^{\delta/\delta}$ HSCs clearly demonstrate that although steady-state hematopoiesis can be maintained, HSCs that are not able to up-regulate *Vegfa* in response to hypoxia are less fit and perform poorly when challenged. Since it has previously been demonstrated that the role VEGFA plays in HSCs is mainly to mediate survival, we suggest that a hypoxia-driven *Vegfa* boost is needed for survival when HSCs seed their new niches after transplantation, while base-line levels of VEGFA together with other factors present in the BM is enough to maintain HSCs in unchallenged mice. However, it cannot be ruled out that processes like homing and lodging are responsible for the observed results. Since normal levels of VEGFA are present in BM of wt recipient mice, our results confirm that the need for VEGFA is indeed HSC intrinsic as previously suggested [35].

Based on ROS staining, the discrepancy between phenotypic and functional HSCs in *Vegfa*$^{\delta/\delta}$ mice could not be explained by the existence of two separate populations within the LSK CD34$^-$ compartment where normoxic HSCs selectively expand to compensate for lower survival of hypoxic HSCs. Rather, both ROS^{lo} and ROS^{hi} LSK CD34$^-$ cells tend to be increased and both these populations have somewhat decreased *Vegfa* expression. It is possible that oxygen/ROS levels in the LSK compartment is already relatively low compared to more mature cells in the BM and this could be one reason why we could not detect differences in *Vegfa* expression between ROS subpopulations. Low ROS levels selects for primitive cells when lineage$^-$ CD45$^+$ cells are used as starting material, indicating that these cells are hypoxic but whether ROS content correlates with oxygen concentration in populations further enriched for HSCs is not clear [13]. Alternatively, ROS might not be a good indicator of oxygen concentration in general. Evidence exists that hypoxia can induce ROS and that ROS is even required for hypoxic signaling [44]. We believe that the increased frequency of HSCs in *Vegfa*$^{\delta/\delta}$ mice is a sign of a stressed situation in the hematopoietic system. Despite the lack of hypoxic *Vegfa* induction, these HSCs survive if unchallenged, but have a severe disadvantage when competing against wt HSCs.

In young *Vegfa*$^{\delta/\delta}$ mice we observed that the epiphyseal growth plate of femur, where endochondral ossification takes place, was diminished. This discovery fits well with a previously described role of VEGFA in the process where chondrocytes in hyaline cartilage proliferates and provides the scaffold for bone formation [45]. This process has also been connected to hypoxia and HIF-activity [46-47]. The volume of bone, and consequently the amount of available endosteal surfaces constituting HSC niches, is well known to affect HSC numbers. Therefore, the ossification phenotype discovered here could possibly influence the HSC phenotype. However, we could not reveal any obvious loss of trabecular bone. Since our analysis showed an increase in HSC numbers rather than a decrease, it is not likely that the reduced ossification have affected HSCs. Still, the defect in endochondral bone formation could be a reason why *Vegfa*$^{\delta/\delta}$ mice are growth arrested since the length of bones should be reduced when bone growth is impaired.

Whether hypoxic HSC niches also exist in the FL remains unknown. FL hematopoiesis peaks around embryonic day 15 in the mouse, and thereafter HSCs start to migrate from the FL to the BM cavities, where hematopoiesis continues during young and adult life. As in adult BM, a decrease in cellularity was observed in FL from *Vegfa*$^{\delta/\delta}$ mice compared to wt. Correspondingly, FL from *Vegfa*$^{\delta/\delta}$ mice contained a higher frequency of both LSK and LSK CD150$^+$ cells. Again, it is possible that this increase in HSPCs is a way to compensate so that efficient hematopoietic output can be maintained in the FL despite inferior HSC survival. Oosthuyse *et al*. reported that the *Vegfa*$^{\delta/\delta}$ mutation causes an approximately 60% prenatal lethality and we show here that this lethality increases to 76% when C57Bl/6 is added to the strain background and 100% when the background approaches pure C57Bl/6. However, neither the cause, nor the time point for this lethality was previously examined although suggested to be caused by insufficient vascular growth. The observation that an increase in the C57Bl/6 contribution increases lethality, suggests that expression patterns of *Vegfa* differs between mouse strains and that a critical threshold level is needed for survival. Indeed, inter-strain differences

in base-line *Vegfa* expression levels have been documented [48]. We show here that a major part of embryonic lethality takes place during a time window from embryonic day 15.5 until birth. Taking into account the competitive-repopulation assay results of adult HSCs, where $Vegfa^{\delta/\delta}$ HSCs have reduced repopulation capacity compared to wt, it is interesting to speculate that $Vegfa^{\delta/\delta}$ FL HSCs would have a similar defect. The process of HSC reconstitution upon transplantation, where HSCs need to successfully migrate to and subsequently survive in BM niches, is likely similar to what is taking place when FL HSCs populate BM niches. Our data raise the possibility that hypoxic regulation of *Vegfa* is involved in seeding of HSCs from FL to BM, although further investigations are needed to prove this.

Takubo *et al*. reported that *Vegfa* levels in HSCs from *Hif1a* conditional knock-out mice were not statistically significantly decreased [29], excluding *Vegfa* as an important mediator of the phenotype in *Hif1a* deficient HSCs. However, redundancy by other HIF variants compensating for the loss of *Hif1a,* as well as biologic effects of undetectable changes in *Vegfa* concentrations, cannot be disqualified. Deletion of the HRE in the *Vegfa* promoter in $Vegfa^{\delta/\delta}$ mice should efficiently abrogate binding of all HIF-variants to the *Vegfa* promoter. We confirmed this in our system by measuring *Vegfa* mRNA levels in hematopoietic cells after hypoxic exposure *in vitro*. While hypoxic up-regulation of *Vegfa* was perturbed in $Vegfa^{\delta/\delta}$ mice, baseline expression was clearly detected. Other documented regulators of *Vegfa* expression include Estrogen [49] and *Ppargc1a* [50]. *Vegfa* is needed for several developmental processes other than hematopoiesis. It is therefore possible that the presence of the $Vegfa^{\delta/\delta}$ mutation during development selects for individuals where *Vegfa* expression unrelated to hypoxia is high, in this way blunting the effect of the mutation in mice that survive past birth. This selection might be a reason for the relative weak phenotype observed in unchallenged mice.

Taken together, although HSPC numbers and differentiation capacity are affected in developing and adult $Vegfa^{\delta/\delta}$ mice, unchallenged hematopoiesis is maintained up to 16 weeks of age. However, in a situation of stress, such as recovery after HSC transplantation, hypoxia/HIF-driven *Vegfa* up-regulation is clearly needed. In conclusion, we demonstrate here a novel role of the hypoxic HSC niche. Together with previously described roles of hypoxia, like balancing quiescence and protecting HSCs against ROS, we have shown that one important function of the hypoxic HSC niche is to provide HSCs intrinsically with the survival factor VEGFA.

Acknowledgements

We thank Håkan Axelson, Stefan Karlsson, Jonas Larsson and Thomas Blom for critical discussions and all the members of the Division of Molecular Medicine and Gene Therapy for help and discussion. We also thank Zhi Ma for FACS cell sorting, Elise Nilsson for excellent immunohistochemical staining and the BMC animal facility staff for taking care of mice. This work was supported by the Swedish Research Council (#K2007-64X-20412-01-3, Linneaus center of excellence grant), the ALF (avtal om läkarutbildning och forskning) grant from Skåne University hospital, and the Åke Wiberg stiftelse to J.C and the Longterm structural Methusalem funding (Flemish Government); Federal Government IUAP Program (P06/30) to P.C.

Authorship

M.R. designed and performed experiments, analyzed data and wrote the manuscript. A.O. and K.R. performed experiments. The $Vegfa^{\delta/\delta}$ mice were generated by P.C. E.D. and G.L. assisted in designing and performing immunohistochemical experiments. J.C. directed research, designed experiments and contributed to writing the manuscript.

Conflict-of-interest disclosure: The authors declare no competing financial interests.

References

1. Calvi, L.M., *et al.* Osteoblastic cells regulate the haematopoietic stem cell niche. *Nature* **425**, 841-846 (2003).

2. Zhang, J., *et al.* Identification of the haematopoietic stem cell niche and control of the niche size. *Nature* **425**, 836-841 (2003).

3. Kiel, M.J., Yilmaz, O.H., Iwashita, T., Terhorst, C. & Morrison, S.J. SLAM family receptors distinguish hematopoietic stem and progenitor cells and reveal endothelial niches for stem cells. *Cell* **121**, 1109-1121 (2005).

4. Sugiyama, T., Kohara, H., Noda, M. & Nagasawa, T. Maintenance of the hematopoietic stem cell pool by CXCL12-CXCR4 chemokine signaling in bone marrow stromal cell niches. *Immunity* **25**, 977-988 (2006).

5. Nilsson, S.K., Johnston, H.M. & Coverdale, J.A. Spatial localization of transplanted hemopoietic stem cells: inferences for the localization of stem cell niches. *Blood* **97**, 2293-2299 (2001).

6. Sipkins, D.A., *et al.* In vivo imaging of specialized bone marrow endothelial microdomains for tumour engraftment. *Nature* **435**, 969-973 (2005).

7. Lo Celso, C., *et al.* Live-animal tracking of individual haematopoietic stem/progenitor cells in their niche. *Nature* **457**, 92-96 (2009).

8. Zhang, C.C. & Lodish, H.F. Insulin-like growth factor 2 expressed in a novel fetal liver cell population is a growth factor for hematopoietic stem cells. *Blood* **103**, 2513-2521 (2004).

9. Dello Sbarba, P., Cipolleschi, M.G. & Olivotto, M. Hemopoietic progenitor cells are sensitive to the cytostatic effect of pyruvate. *Exp Hematol* **15**, 137-142 (1987).

10. Harrison, J.S., Rameshwar, P., Chang, V. & Bandari, P. Oxygen saturation in the bone marrow of healthy volunteers. *Blood* **99**, 394 (2002).

11. Parmar, K., Mauch, P., Vergilio, J.A., Sackstein, R. & Down, J.D. Distribution of hematopoietic stem cells in the bone marrow according to regional hypoxia. *Proc Natl Acad Sci U S A* **104**, 5431-5436 (2007).

12. Winkler, I.G., *et al.* Positioning of bone marrow hematopoietic and stromal cells relative to blood flow in vivo: serially reconstituting hematopoietic stem cells reside in distinct nonperfused niches. *Blood* **116**, 375-385 (2010).

13. Jang, Y.Y. & Sharkis, S.J. A low level of reactive oxygen species selects for primitive hematopoietic stem cells that may reside in the low-oxygenic niche. *Blood* **110**, 3056-3063 (2007).

14. Levesque, J.P., *et al.* Hematopoietic progenitor cell mobilization results in hypoxia with increased hypoxia-inducible transcription factor-1 alpha and vascular endothelial growth factor A in bone marrow. *Stem Cells* **25**, 1954-1965 (2007).

15. Kubota, Y., Takubo, K. & Suda, T. Bone marrow long label-retaining cells reside in the sinusoidal hypoxic niche. *Biochem Biophys Res Commun* **366**, 335-339 (2008).

16. Eliasson, P., Karlsson, R. & Jönsson, J.-I. Hypoxia expands primitive hematopoietic progenitor cells from mouse bone marrow during in vitro culture and preserves the colony-forming ability. *Journal of stem cells* **1**, 247-257 (2006).

17. Danet, G.H., Pan, Y., Luongo, J.L., Bonnet, D.A. & Simon, M.C. Expansion of human SCID-repopulating cells under hypoxic conditions. *J Clin Invest* **112**, 126-135 (2003).

18. Cipolleschi, M.G., Dello Sbarba, P. & Olivotto, M. The role of hypoxia in the maintenance of hematopoietic stem cells. *Blood* **82**, 2031-2037 (1993).

19. Cipolleschi, M.G., *et al.* Severe hypoxia enhances the formation of erythroid bursts from human cord blood cells and the maintenance of BFU-E in vitro. *Exp Hematol* **25**, 1187-1194 (1997).

20. Ivanovic, Z., Dello Sbarba, P., Trimoreau, F., Faucher, J.L. & Praloran, V. Primitive human HPCs are better maintained and expanded in vitro at 1 percent oxygen than at 20 percent. *Transfusion* **40**, 1482-1488 (2000).

21. Ivanovic, Z., *et al.* Simultaneous maintenance of human cord blood SCID-repopulating cells and expansion of committed progenitors at low O2 concentration (3%). *Stem Cells* **22**, 716-724 (2004).

22. Shima, H., *et al.* Reconstitution activity of hypoxic cultured human cord blood CD34-positive cells in NOG mice. *Biochem Biophys Res Commun* **378**, 467-472 (2009).

23. Wang, G.L., Jiang, B.H., Rue, E.A. & Semenza, G.L. Hypoxia-inducible factor 1 is a basic-helix-loop-helix-PAS heterodimer regulated by cellular O2 tension. *Proc Natl Acad Sci U S A* **92**, 5510-5514 (1995).

24. Wang, G.L. & Semenza, G.L. Purification and characterization of hypoxia-inducible factor 1. *J Biol Chem* **270**, 1230-1237 (1995).

25. Ema, M., *et al.* A novel bHLH-PAS factor with close sequence similarity to hypoxia-inducible factor 1alpha regulates the VEGF expression and is potentially involved in lung and vascular development. *Proc Natl Acad Sci U S A* **94**, 4273-4278 (1997).

26. Jaakkola, P., *et al.* Targeting of HIF-alpha to the von Hippel-Lindau ubiquitylation complex by O2-regulated prolyl hydroxylation. *Science* **292**, 468-472 (2001).

27. Bruick, R.K. & McKnight, S.L. A conserved family of prolyl-4-hydroxylases that modify HIF. *Science* **294**, 1337-1340 (2001).

28. Ivan, M., *et al.* HIFalpha targeted for VHL-mediated destruction by proline hydroxylation: implications for O2 sensing. *Science* **292**, 464-468 (2001).

29. Takubo, K., *et al.* Regulation of the HIF-1alpha level is essential for hematopoietic stem cells. *Cell Stem Cell* **7**, 391-402 (2010).

30. Eliasson, P., *et al.* Hypoxia mediates low cell-cycle activity and increases the proportion of long-term-reconstituting hematopoietic stem cells during in vitro culture. *Exp Hematol* **38**, 301-310 (2010).

31. Shweiki, D., Itin, A., Soffer, D. & Keshet, E. Vascular endothelial growth factor induced by hypoxia may mediate hypoxia-initiated angiogenesis. *Nature* **359**, 843-845 (1992).

32. Plate, K.H., Breier, G., Weich, H.A. & Risau, W. Vascular endothelial growth factor is a potential tumour angiogenesis factor in human gliomas in vivo. *Nature* **359**, 845-848 (1992).

33. Ferrara, N., *et al.* Heterozygous embryonic lethality induced by targeted inactivation of the VEGF gene. *Nature* **380**, 439-442 (1996).

34. Carmeliet, P., *et al.* Abnormal blood vessel development and lethality in embryos lacking a single VEGF allele. *Nature* **380**, 435-439 (1996).

35. Gerber, H.P., *et al.* VEGF regulates haematopoietic stem cell survival by an internal autocrine loop mechanism. *Nature* **417**, 954-958 (2002).

36. Chan, C.K., *et al.* Endochondral ossification is required for haematopoietic stem-cell niche formation. *Nature* **457**, 490-494 (2009).

37. Hooper, A.T., *et al.* Engraftment and reconstitution of hematopoiesis is dependent on VEGFR2-mediated regeneration of sinusoidal endothelial cells. *Cell Stem Cell* **4**, 263-274 (2009).

38. Oosthuyse, B., *et al.* Deletion of the hypoxia-response element in the vascular endothelial growth factor promoter causes motor neuron degeneration. *Nat Genet* **28**, 131-138 (2001).

39. Ohnishi, S., Yasuda, T., Kitamura, S. & Nagaya, N. Effect of hypoxia on gene expression of bone marrow-derived mesenchymal stem cells and mononuclear cells. *Stem Cells* **25**, 1166-1177 (2007).

40. Simsek, T., *et al.* The distinct metabolic profile of hematopoietic stem cells reflects their location in a hypoxic niche. *Cell Stem Cell* **7**, 380-390 (2010).

41. Hock, H., *et al.* Gfi-1 restricts proliferation and preserves functional integrity of haematopoietic stem cells. *Nature* **431**, 1002-1007 (2004).

42. Nie, Y., Han, Y.C. & Zou, Y.R. CXCR4 is required for the quiescence of primitive hematopoietic cells. *J Exp Med* **205**, 777-783 (2008).

43. de Haan, G. & Van Zant, G. Intrinsic and extrinsic control of hemopoietic stem cell numbers: mapping of a stem cell gene. *J Exp Med* **186**, 529-536 (1997).

44. Hamanaka, R.B. & Chandel, N.S. Mitochondrial reactive oxygen species regulate hypoxic signaling. *Curr Opin Cell Biol* **21**, 894-899 (2009).

45. Gerber, H.P., *et al.* VEGF couples hypertrophic cartilage remodeling, ossification and angiogenesis during endochondral bone formation. *Nat Med* **5**, 623-628 (1999).

46. Saito, T., *et al.* Transcriptional regulation of endochondral ossification by HIF-2alpha during skeletal growth and osteoarthritis development. *Nat Med* **16**, 678-686 (2010).

47. De Spiegelaere, W., Cornillie, P., Casteleyn, C., Burvenich, C. & Van den Broeck, W. Detection of hypoxia inducible factors and angiogenic growth factors during foetal endochondral and intramembranous ossification. *Anat Histol Embryol* **39**, 376-384 (2010).

48. Li, Q., Michaud, M., Stewart, W., Schwartz, M. & Madri, J.A. Modeling the neurovascular niche: murine strain differences mimic the range of responses to chronic hypoxia in the premature newborn. *J Neurosci Res* **86**, 1227-1242 (2008).

49. Mueller, M.D., *et al.* Regulation of vascular endothelial growth factor (VEGF) gene transcription by estrogen receptors alpha and beta. *Proc Natl Acad Sci U S A* **97**, 10972-10977 (2000).

50. Arany, Z., *et al.* HIF-independent regulation of VEGF and angiogenesis by the transcriptional coactivator PGC-1alpha. *Nature* **451**, 1008-1012 (2008).

Tables

Table 1. Genotype distribution from δ/+ x δ/+ matings.

Genotype	Mendelian, %	Born, % n=454	Day 15.5, % n=104
wt	25	34	26
δ/+	50	60	56
δ/δ	25	6	18

Figures

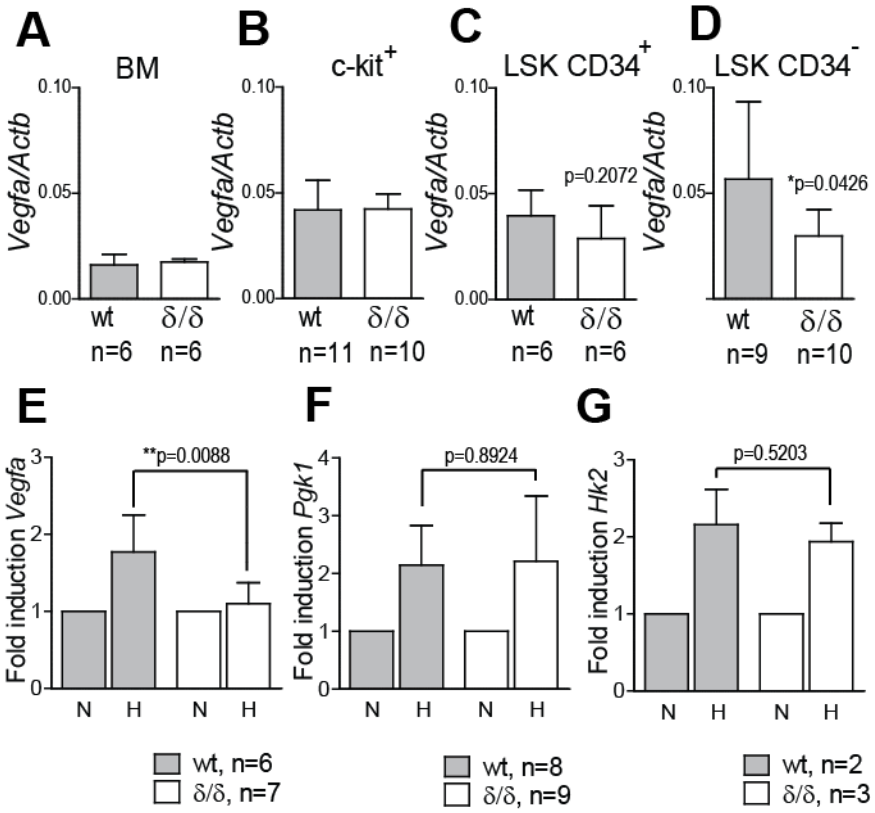

Figure 1. *Vegfa* expression is reduced in LSK CD34$^-$ cells from *Vegfa*$^{\delta/\delta}$ BM but not in more differentiated BM cells. *Vegfa* expression was measured by Q-RT-PCR in (**A**) unfractionated BM, (**B**) c-kit enriched cells (**C**) LSK CD34$^+$ cells (p=0.2072, t-test) and (**D**) LSK CD34$^-$ cells (*p=0.0426, t-test) from *Vegfa*$^{\delta/\delta}$ or wt mice. *Vegfa* expression was normalized to *Actb* expression. Bars represent mean ±SD. mRNA levels of (**E**) *Vegfa* (*p=0.0088, t-test) (**F**) *Pgk1* (p=0.8924, t-test) and (**G**) *Hk2* (p=0.5203, t-test) was measured in c-kit enriched cells from *Vegfa*$^{\delta/\delta}$ or wt mice previously incubated in normoxic or hypoxic conditions for 12 hours. Data in E-G are presented as fold increase in gene expression compared to normoxia. Bars represent mean ±SD. Results shown are data combined from 3 independent experiments. (N=normoxia, H=hypoxia).

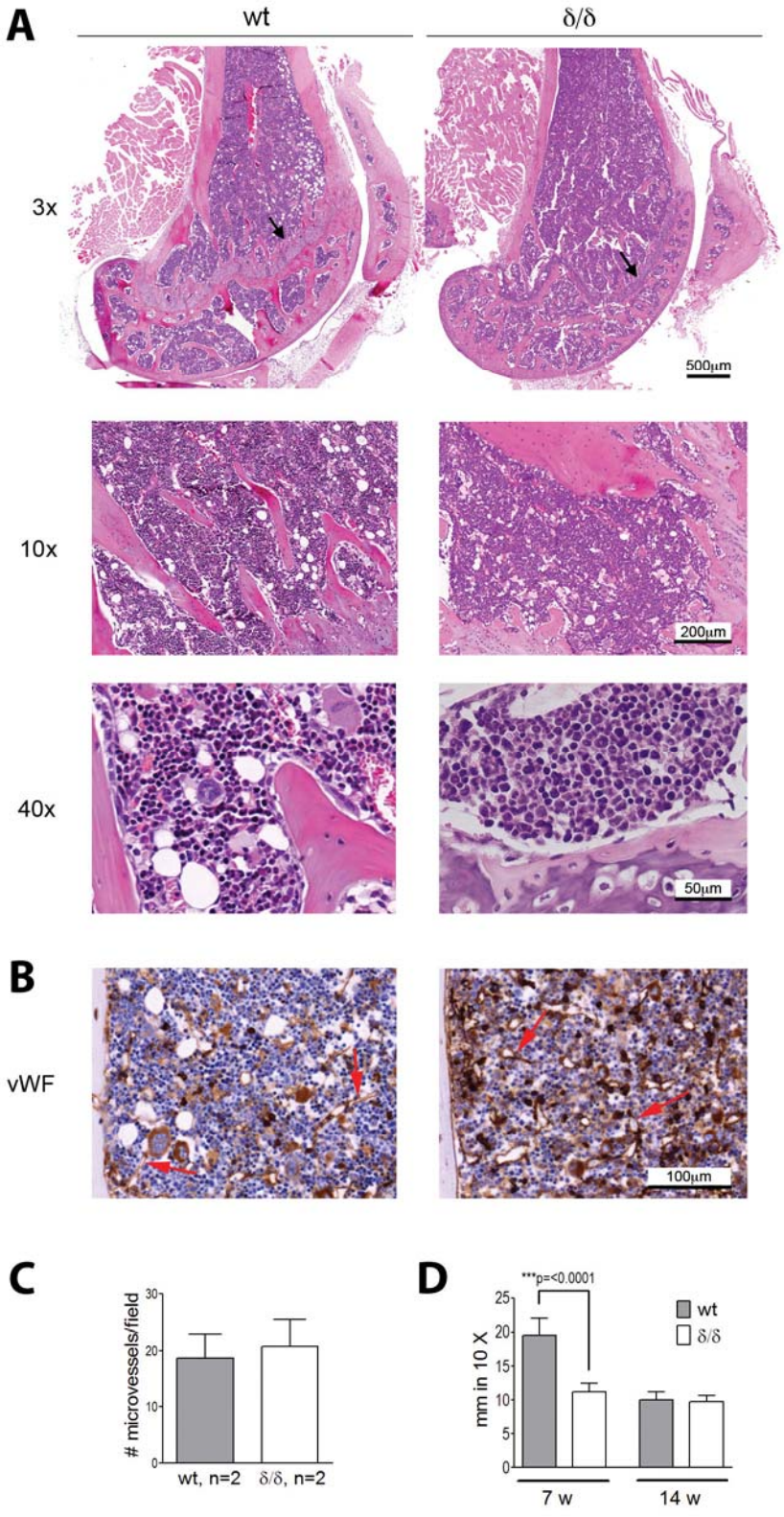

Figure 2. BM morphology and microvessel density of *Vegfa*$^{\delta/\delta}$ mice are normal while the endochondral ossification is decreased. (**A**) Representative histology images of mouse BM sections were captured from 1 wt mouse and 2 *Vegfa*$^{\delta/\delta}$ mice in the trabecular area of distal femur samples at original magnification x3, x10 and x40. Histological specimens were stained with hematoxylin and eosin. Arrows indicate the epiphyseal growth plate. (**B**) BM sections were immunohistochemically stained with vWF to detect microvessels. Original magnification x20. Red arrows indicate microvessels. (**C**) The average number of microvessels was counted in 3 different images per mouse captured from 2 mice per group. Bars represent mean ±SD. (**D**) The thickness of the epiphyseal growth plate in femur was measured manually in 10x magnifications. Bars represent mean ±SD of 7–11 measurements from representative images, $p<0.0001$, t-test. All images were captured using a Zeiss slide scanner containing a Sony DFW-X710 camera and MIRAX software.

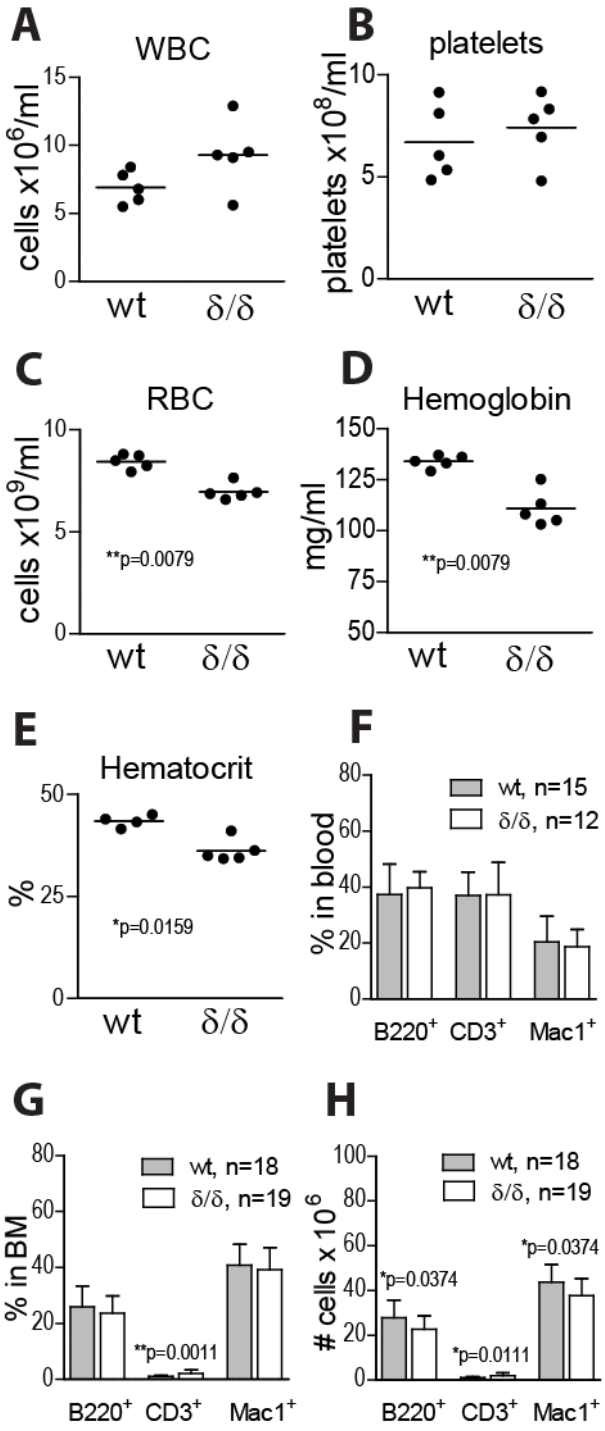

Figure 3. *Vegfa*$^{\delta/\delta}$ mice display mild anemia and altered numbers of differentiated cells in the BM. (**A**) WBC count, (**B**) platelet count (**C**) RBC count, (**D**) hemoglobin, and (**E**) hematocrit levels were measured on blood samples from *Vegfa*$^{\delta/\delta}$ or wt mice. Results are shown from 5 individual mice per group. P-values are from Mann-Whitney test. (**F**) Percentages of B220$^+$, CD3$^+$, and Mac-1$^+$ cells in PB were determined by FACS analysis. Bars represent mean ±SD. Results shown are data combined from 5 independent experiments. (**G**) BM lineage distribution. Bars represent mean ±SD, **p=0.0011, Mann-Whitney test. (**H**) Total numbers of B220$^+$, CD3$^+$, and Mac-1$^+$ cells in 2 x femur and tibia. Bars represent mean ±SD, p-values are from Mann-Whitney test. Results shown in G and H are data combined from 6 independent experiments.

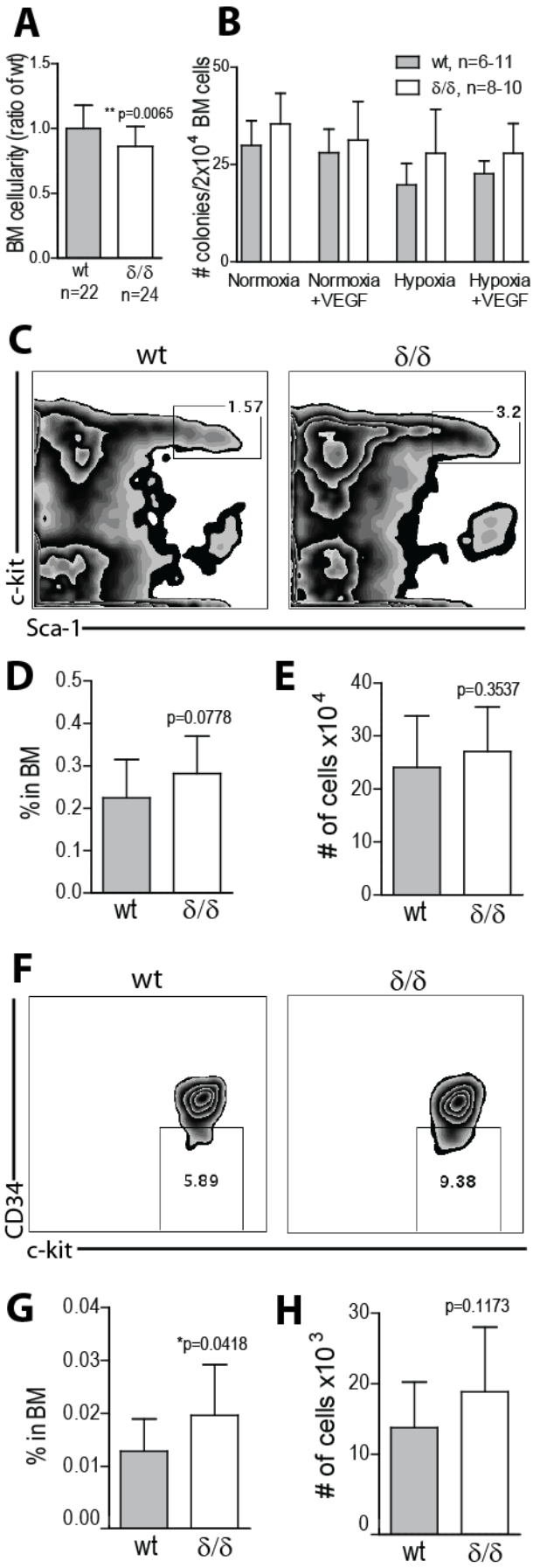

Figure 4. HSPC frequency is increased in BM with defect hypoxia-regulated *Vegfa* expression. (A) BM cellularity was determined by counting mononuclear cells from femur, tibia and iliac crest from *Vegfa*$^{\delta/\delta}$ or wt mice. Data are presented as ratio of wt BM cellularity and results shown are combined data from 8 independent experiments. Bars represent mean ±SD, **p=0.0065, t-test. **(B)** Total CFU frequency was measured by plating 2x10^4 BM cells/mL in methylcellulose, with or without mVEGFA, followed by incubation in normoxia or hypoxia for 7 days. Results shown are data combined from 4 independent experiments. **(C)** The frequency of LSK cells in the BM was measured by FACS analysis. Representative FACS plots of lineage$^-$ gated cells (**D**) Percentage LSK cells in BM. **(E)** Total number of LSK cells per 2 x femur and tibia. Results shown in D-E are data combined from 5 independent experiments. Bars represent mean ±SD, n=15-17 mice per genotype. P-values are from t-test. (**F**) The frequency of LSK CD34$^-$ cells in BM was measured by FACS analysis. Representative FACS plots of LSK gated cells. (**G**) Percentage LSK CD34$^-$ cells in BM. (**H**) Total number of LSK CD34$^-$ cells per 2 x femur and tibia. Results shown in G-H are data combined from 4 independent experiments. Bars represent mean ±SD, n=13 mice per genotype. P-values are from t-test.

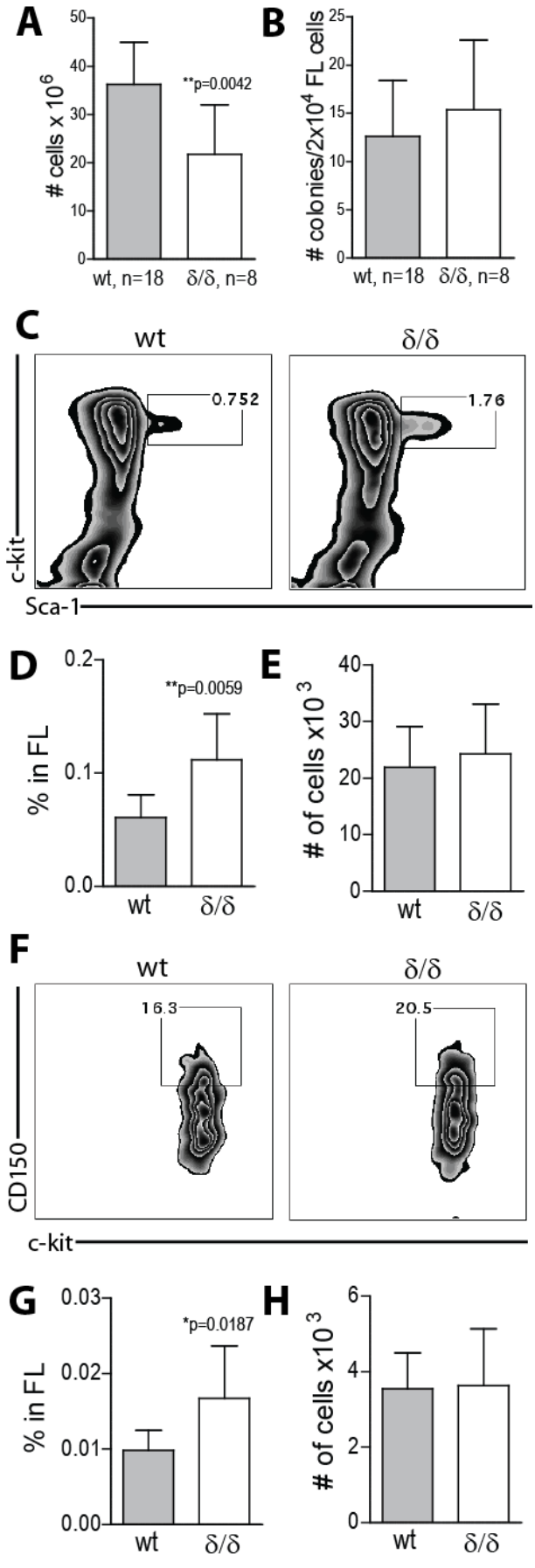

Figure 5. HSPC frequency is increased in FL cells lacking hypoxic *Vegfa* induction. (A) FL cellularity of *Vegfa*$^{\delta/\delta}$ or wt mice. Results shown are combined data from 5 independent experiments. Bars represent mean ±SD, **p=0.0042 Mann-Whitney test. **(B)** Total CFU frequency was measured by plating 2x10^4 FL cells/mL in methylcellulose followed by incubation in normoxia for 7 days. Results shown are data combined from 4 independent experiments. **(C)** The frequency of LSK cells in FL was measured by FACS analysis. Representative FACS plots of lineage$^-$ gated cells. (**D**) Percentage LSK cells in FL. **p=0.0059, t-test. **(E)** Total number of LSK cells per FL. (**F**) The frequency of LSK CD150$^+$ cells in FL was measured by FACS analysis. Representative FACS plots of LSK gated cells are shown. (**G**) Percentage LSK CD150$^+$ cells in FL. *p=0.0187, t-test. (**H**) Total number of LSK CD150$^+$ cells per FL. Results shown in C-H are data combined from 4 independent experiments. Bars represent mean ±SD, n=8–9 mice per genotype.

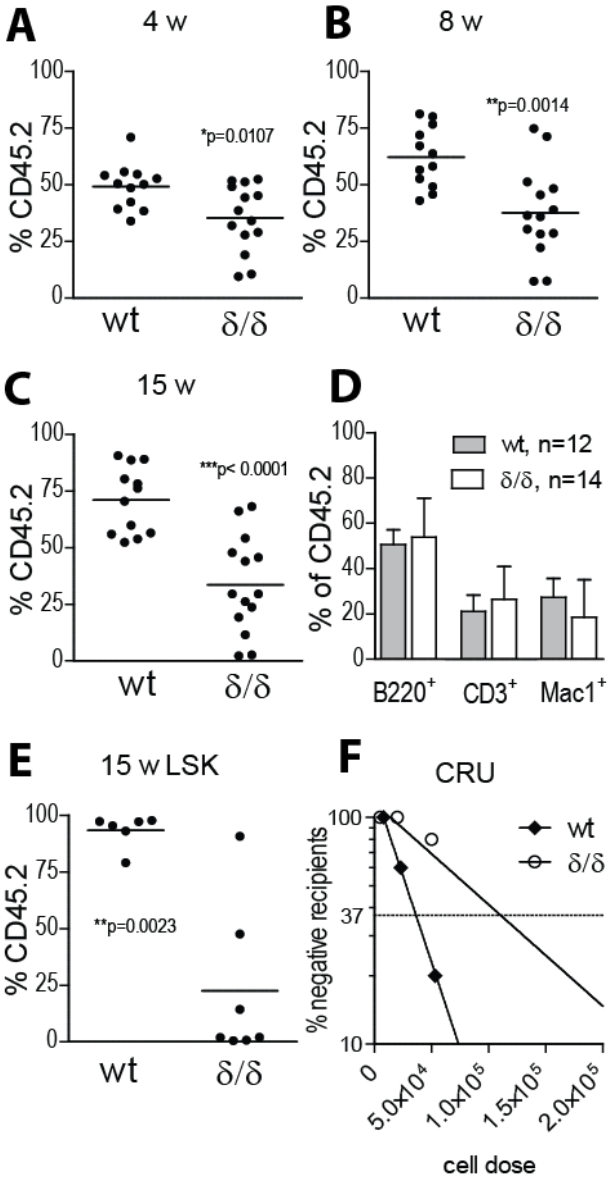

Figure 6. HSCs lacking hypoxia-induced *Vegfa* expression have impaired competitive reconstitution potential. $2x10^5$ test cells (CD45.2) and $2x10^5$ competitor cells (CD45.1) were transplanted to lethally irradiated recipients. Results are shown from 1 representative experiment out of 2 performed where 3 different donors per genotype were injected into 4–5 recipients each. Test cell contribution to PB at (**A)** 4 weeks, *p=0.0107, t-test (**B**) 8 weeks, **p=0.0014, t-test, and (**C**) 15 weeks post transplantation, ***p<0.0001, t-test. (**D**) Lineage distribution of engrafted cells in PB at 15 weeks post transplantation. Bars represent mean ±SD. (**E**) Test cell contribution to the BM LSK compartment at 15 weeks post transplantation. **p=0.0023, Mann-Whitney test. (**F**) CRU frequency was determined by limiting-dilution transplantations. Percentages of recipients with negative engraftment of test cells are plotted against the cell dose given. n=5 recipient mice per cell dose and n=3 donors per genotype. Poisson distribution gives that 1 CRU is present at the derived cell dose where the frequency of negatively engrafted recipients is 37%.

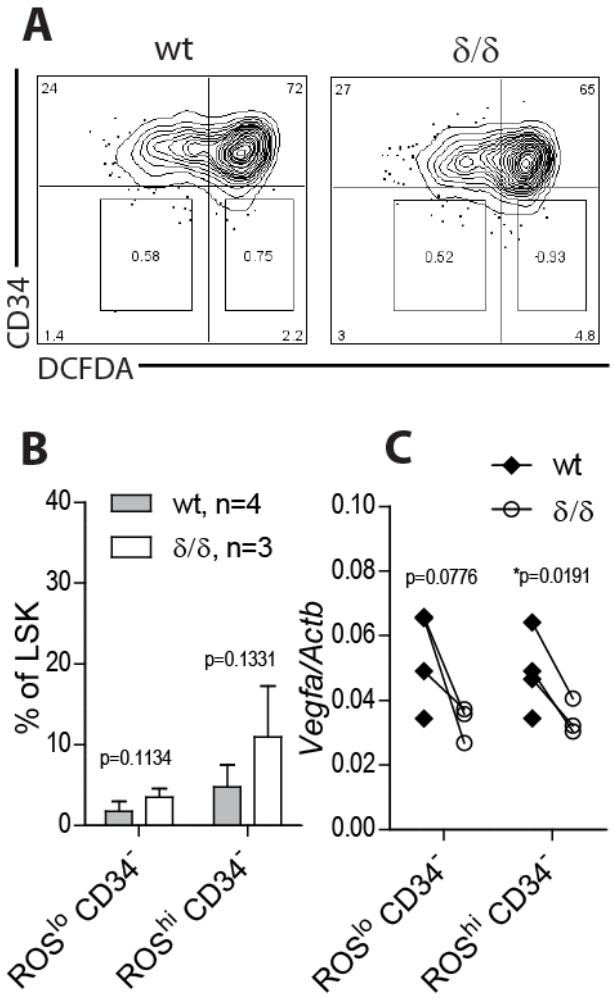

Figure 7. *Vegfa* expression in ROS^{lo} and ROS^{hi} HSC populations. BM cells from *Vegfa*$^{\delta/\delta}$ or wt mice were stained with markers to detect LSK CD34 and DCFDA to detect ROS. (**A**) Representative FACS profiles of LSK gated cells showing gates used for sorting of CD34$^-$ ROS^{lo} and CD34$^-$ ROS^{hi} populations. (**B**) Percentage LSK CD34$^-$ ROS^{lo} and LSK CD34$^-$ ROS^{hi} cells within LSK gated cells. Bars represent mean ±SD. P-values are from t-test. (**C**) *Vegfa* expression in sorted subpopulations. Each dot represents an individual mouse and connecting lines are between littermate pairs. P-values are from paired t-test. Results shown are data combined from 2 independent experiments.

Supplementary Methods

Cells

PB and BM samples were taken from 6–16 week old *Vegfa*$^{\delta/\delta}$ and wt mice or recipient mice previously receiving BM transplantation. PB samples were taken by tail vein bleeding in 2500 IE/KY/mL Heparin (Leo Pharma, Malmö, Sweden) followed by red cell lysis in NH_4Cl (STEMCELL Technologies, Vancouver). BM was harvested by crushing femur, tibia and/or iliac crest in phosphate buffered saline (PBS) containing 2% Fetal Calf Serum (FCS) (Invitrogen, Carlsbad, CA) and passaged through a 70-µm strainer (BD Bioscience, San Jose, CA). FLs were dissected from fetuses of 15.5 day pregnant females and put in PBS containing 2% FCS. Single-cell suspensions were obtained by passing the livers through 23-gauge needles, followed by filtering through a 70-µm strainer.

Cell Culture

For colony forming unit (CFU) assays, BM or FL cells were plated at a concentration of $2x10^4$ cells/mL in methylcellulose M3234 (STEMCELL Technologies), supplemented with 20% Iscove's modified Dulbecco's medium (Invitrogen), 1000 U/mL penicillin, 1000 µM streptomycin (Invitrogen), 50 ng/mL murine stem cell factor, 10 ng/mL murine interleukin-3, 50 ng/mL human interleukin-6 and 5 U/mL erythropoietin (Janssen Cilag, Sollentuna, Sweden) (all cytokines from Peprotech, London, United Kingdom if nothing else stated). In some cases, murine VEGFA (mVEGFA) (Peprotech) was added to the cultures. Plates were incubated in normoxia in a humidified 5% CO_2 incubator at 37°C or in hypoxia (1% O_2) in a humidified 5% CO_2 In$Vivo_2$ Hypoxia Work station 400 (Ruskinn Technology Ltd, United Kingdom) at 37°C and colonies were counted on day 7. For analysis of hypoxia-induced gene expression, c-kit enriched cells were plated in StemSpan SFEM (STEMCELL Technologies) supplemented with 1000 U/mL penicillin, 1000 µM streptomycin, 50 ng/mL murine stem cell factor, 50 ng/mL human Flt-3L and 50 ng/mL human thrombopoietin (Peprotech) and incubated for 12 hours in normoxia or hypoxia as described above.

Antibodies for Flow Cytometry

Antibodies (Biolegend, San Diego) from the following clones were used: B220 (RA3-6B2), CD3ε (145-2C11), Mac-1 (M1/70), c-kit (2B8), CD150 (TC15-12F12.2), Sca-1 (E13-161.7), Gr-1 (RB6-8C5), CD4 (RM4-4), CD5 (53-7.3), CD8 53-6.7), Ter119 (Ter119), CD45.1 (A20), CD45.2 (104). CD34 (RAM34) was purchased from BD Bioscience.

Histology and Immunohistochemistry

Femur and tibia were fixed in a PBS-buffered 4% paraformaldehyde solution (Sigma-Aldrich) and then decalcified with 0.5 M EDTA (ethylenediaminetetraacetic acid) for 48 hours. The paraffin-embedded tissue was cut in 4 µm thick sections, deparaffinized using xylene, and rehydrated using descending concentrations of ethanol according to standard protocol. The specimens were treated with Proteinase K (Dako, Glostrup, Denmark) for 10 minutes and stained with anti-rabbit von Willebrand factor (vWF) antibody (1:5000, Abcam, Cambridge, USA) and EnVision FLEX kit using an AutoStainer Plus (Dako) at room temperature. Histological sections were manually stained with hematoxylin-eosin. Digital images were captured using a slide scanner, (Zeiss, Hertfordshire, United Kingdom) containing a Sony DFW-X710 camera and MIRAX software.

Quantitative Real-time PCR

Measurements of *Vegfa* expression were performed on unfractionated BM cells, c-kit$^+$, sorted LSK CD34$^{+/-}$, and/or ROS$^{hi/lo}$ LSK CD34$^{+/-}$ cells. *Vegfa*, *Pgk1,* and *Hk2* expression was measured in c-kit$^+$ cells following culture. Gene expression was normalized to the reference gene β-actin (*Actb).* Total RNA was extracted by RNeasy Micro or Mini kit (Qiagen, Hilden, Germany) according to instructions from the manufacturer. cDNA was synthesized using random-hexamer primers (Fermentas, Helsingborg, Sweden) and Superscript III Reverse transcriptase (Invitrogen). Quantitative real-time PCR **(**Q-RT-PCR) reactions were performed on a LightCycler system (Roche, Stockholm, Sweden) with 1:12000 dilution of SybrGreen, 1 mg/mL BSA (Sigma-Aldrich), 0.5 mM forward and reverse

primers, 0.8 mM dNTPs, 4.5-5.0 mM $MgCl_2$, and 0.5 U/μL Platinum Taq Polymerase (Invitrogen). Forward and reverse primers used for quantification were:
Vegfa 5'-GGAGAGCAGAAGTCCCATGA-3' and 5'-ACACAGGACGGCTTGAAGAT-3';
Pgk1 5'-AGGCTGGTGGATTTTTGATG-3' and 5'-CAGCTGGATCTTGTCTGCAA-3';
Hk2 5'-GACCAGAGCATCCTCCTCAA-3' and 5'-GCTTCCTTCAGCAAGGTGAC-3';
Actb 5'-CATTGTGATGGACTCCGGTGACGG-3' and 5'-CATAGCACAGCTTCTCTTTGATG-3'.

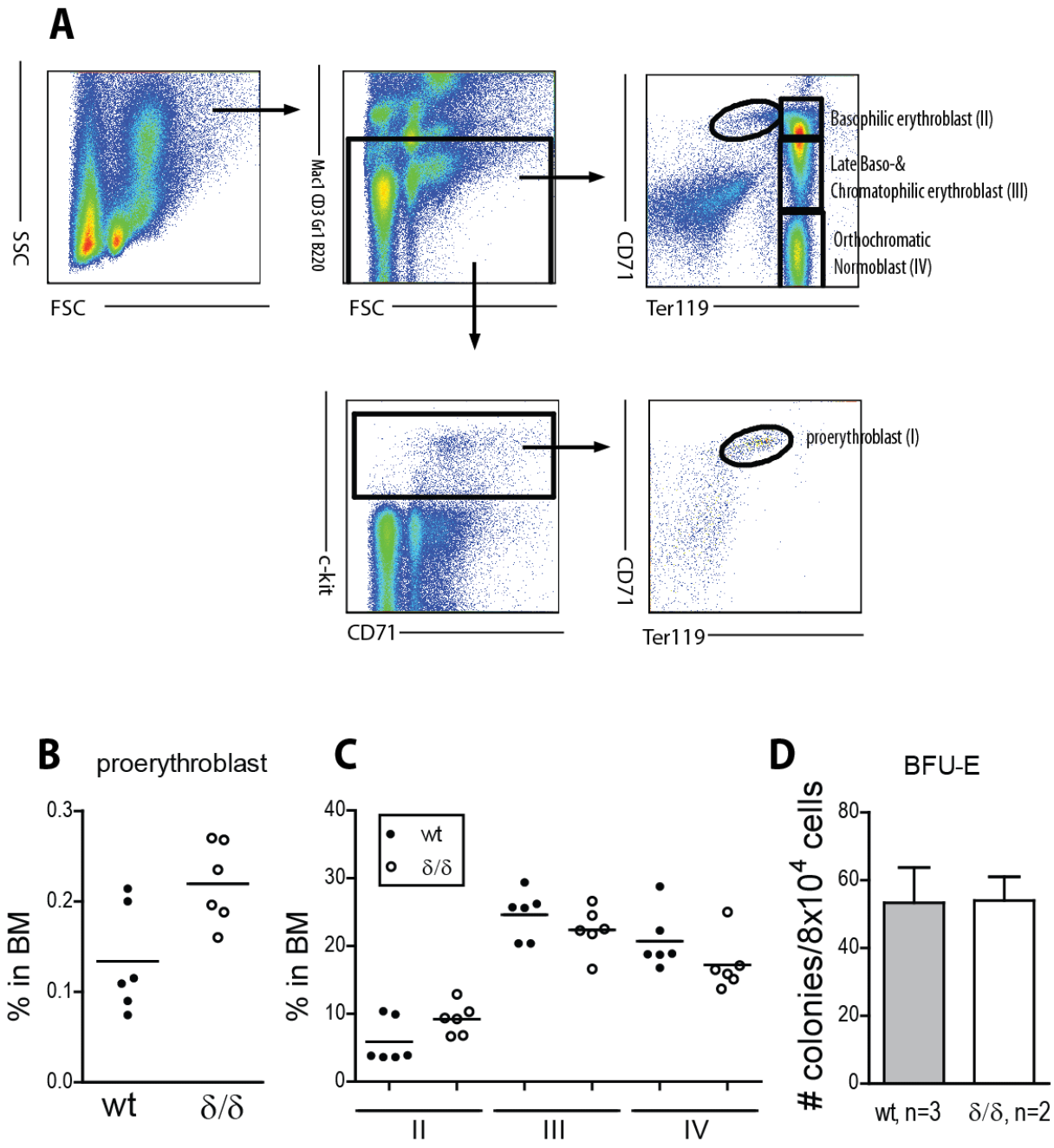

Supplementary Figure 1. For FACS analysis of erythroid progenitors, BM cells from *Vegfa*$^{\delta/\delta}$ or wt were stained with Mac-1-PeCy5, B220-PeCy5, CD3-PeCy5, Gr1-PeCy5, CD71-FITC, c-kit-APC and Ter119-PE. (**A**) Schematic overview of the FACS strategy used. Cells were gated for negative expression of the non-erythroid markers Mac-1, B220, CD3 and Gr-1. Thereafter, basophilic erythroblasts, late baso- and chromatophilic erythroblasts and orthochromatic normoblasts were identified based on CD71 and Ter119 expression. Proerythroblasts were identified by gating on c-kit positive cells expressing CD71 and Ter119. (**B**) Frequency of proerythroblasts in BM. (**C**) Frequency of populations II, III, and IV in BM. Results shown are combined data from 2 independent experiments. (**D**) Erythroid blast forming colonies (BFU-E) were measured by plating BM cells at a concentration of 8 x 10^4 cells/mL in methylcellulose M3436 (STEMCELL Technologies). Data shown is from 1 experiment, representing 3 wt and 2 *Vegfa*$^{\delta/\delta}$ mice. Bars represent mean ±SD.